Thermal Barrier Formation and Plasma Confinement in the Axisymmetrized Tandem Mirror GAMMA 10

M. Inutake, T. Cho, M. Ichimura, K. Ishii, A. Itakura, I. Katanuma, Y. Kiwamoto, Y. Kusama, A. Mase, S. Miyoshi, Y. Nakashima, T. Saito, A. Sakasai, K. Sawada, I. Wakaida, N. Yamaguchi, and K. Yatsu

Plasma Research Center, University of Tsukuba, Ibaraki, 305, Japan

(Received 1 May 1985)

In the axisymmetrized tandem mirror GAMMA 10, thermal-barrier and plug potentials have been formed in the axisymmetric mirror cells at both ends and directly measured with Au neutral-beam probes and end-loss analyzers. Strong end-loss reduction associated with the potential formation results in enhancement of the axial particle confinement time 100 times over the mirror confinement time without plugging, in reasonable agreement with Pastukhov formula. An empirical scaling on nonambipolar radial ion confinement time in the axisymmetrized field configuration is presented.

PACS numbers: 52.55.Jd

Current tandem mirror researches focus on improvement of confinement properties over the original configuration.[1-4] The thermal-barrier[5] formation, for better axial confinement, has been recently demonstrated in the tandem mirror device TMX-U[6] at the quadrupole-end mirror cell. In order to reduce theoretically predicted radial losses[7] associated with asymmetries in confining fields, further improvement is being pursued, in the axisymmetrized tandem mirrors GAMMA 10[8] and TARA,[9] from the viewpoint of axisymmetrization for central-cell ion confinement.

In this Letter, we report the first direct observation of the thermal-barrier potential while the confining plug potential is formed at both ends of the GAMMA 10 and the end-loss fluxes are strongly reduced. This also represents the first experiment that demonstrates the formation of the thermal barrier and the plug potentials in an axisymmetric mirror cell. The axial particle-confinement time scales in good agreement with the Pastukhov formula and an empirical scaling has been obtained on the nonambipolar radial transport with respect to the central-cell potential.

The GAMMA 10 is a minimum-B anchored tandem mirror with outboard thermal-barrier or plug cells.[10] The typical magnetic field configuration with central-cell field intensity of 0.4 T is shown in Fig. 1. The mirror ratios at the central, anchor, and axisymmetric plug or barrier cells are about 5, 3, and 6, respectively. An axisymmetrized field configuration of GAMMA 10 is attributed to the following features. Axisymmetric mirror field at both ends of the central solenoid reduces the fraction of particles passing through the minimum-B region. The geodesic curvature in the region is carefully designed to be antisymmetric with respect to the anchor midplane to minimize net radial drift from a flux surface for the passing particles[10] and at the same time to establish axisymmetric equilibrium by suppressing net parallel current[11] flowing into the central cell. The cancellation of the geodesic curvature effect is effective as long as azimuthal drift is small in the minimum-B region. In order to lower the plasma potential which drives the drift, five concentric, mutually insulated circular plates are installed at each end of GAMMA 10.

Heating systems are as follows: magneto-plasma-dynamic (MPD) guns inject an initial plasma from both ends. Neutral beams (NBI) with 20 kV, 60-A drain, and 41° injection angle and 35 kV, 70-A drain, and 75° injection angle produce sloshing ions in the plug or barrier cells and hot ions in the anchor cells, respectively. Four gyrotrons with 28 GHz, 140 kW are used both to produce magnetically trapped hot electrons near the midplane (second-harmonic electron cyclotron resonance heating, $2\omega_{ce}$ ECRH) and to plug warm electrons at the off-midplane (ω_{ce} resonance). Parabolic reflectors are used for conversion of the

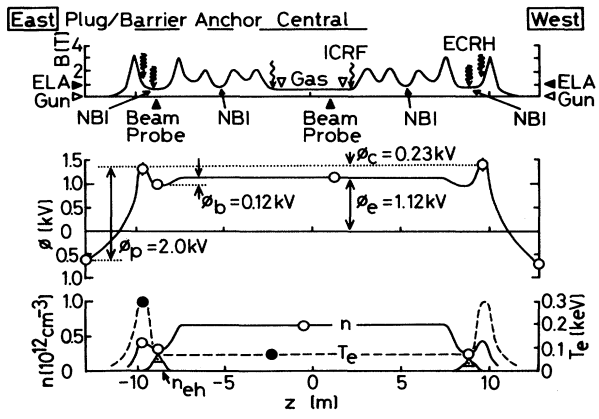

FIG. 1. Axial profiles of (top) magnetic field, (middle) plasma potential, and (bottom) total electron density (open circles), hot-electron density (open triangles), electron temperature (filled circles).

TE_{02} mode to a linearly polarized X mode and for aiming of a 15-cm-diam beam at the resonance surfaces near axis. Ion-cyclotron-resonance heating (ICRH) at 9.6 MHz is used to heat the central-cell ions.

Strong end plugging is demonstrated in Fig. 2. The time squence of the shot is as follows: Following the gun-produced plasma injection and central-cell gas puffing, the sloshing and anchor NBI's and barrier ECRH are injected to build up hot ions and electrons. In a quasisteady phase of the central-cell plasma the plug ECRH is applied to create the plug potentials for axial confinement. During the plug-ECRH pulse, the ion-loss fluxes into end-loss analyzers (ELA) at both ends decrease significantly and a simultaneous increase in the central-cell line density is observed. Active gas puffing is made only in the central cell to minimize charge-exchange losses of hot ions and barrier filling due to neutral-gas ionization. During the strong end plugging, the hydrogen-gas pressures at the plug or barrier, anchor, and central cells are kept less than 1.0×10^{-7}, 2.0×10^{-7}, and 1.0×10^{-6} Torr, respectively. We have observed to date end plugging during 7 ms at central-cell densities as high as 9×10^{11} cm^{-3} and parallel ion temperature $T_{i\parallel}=50$ eV, measured with ELA near the ends without the central-cell ICRH, while with the ICRH, we have observed 10-ms plugging at densities up to 2×10^{12} cm^{-3} and $T_{i\parallel}=200$ eV and perpendicular temperature $T_{i\perp}=500$ eV estimated from diamagnetic signals and by a time-of-flight charge-exchange energy analyzer installed in the central cell.

From pulse-height analyses of the radiated x rays, the barrier hot-electron temperature T_{eh} is found to rise quickly in 1–3 ms and saturate gradually at 30–50 keV. From measurements of x-ray pinhole-camera image, cyclotron emission profile, and diamagnetic signals measured at several axial positions, it is confirmed that the hot-electron density profile is fairly uniform with a half-maximum diameter of 30 cm and an axial extent of 100 cm.[12] The largest fraction of the hot electrons so far obtained is 0.9 with averaged beta value of 5%. In the shot shown in Fig. 2, those values are 0.4 and 1%, respectively. The warm-electron temperature in the plug region is determined to be 300 eV from the measurement of $2\omega_{ce}$ emission intensity and the soft x-ray absorption by polyethylene 2–15 μm in thickness. The central-cell electron temperature estimated from $2\omega_{ce}$ emission is 60–120 eV, depending on the density, during the plug ECRH. This is much lower than the plug temperature. The pitch-angle distribution characterizing sloshing ions is observed with a secondary-emission-detector array,[13] showing a peak at 40° consistent with the neutral-beam injection angle.

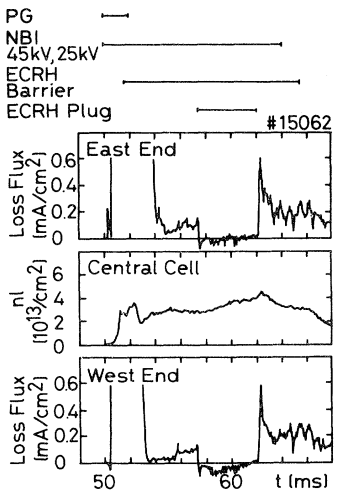

FIG. 2. Time variations of central-cell line density and end-loss fluxes measured near the end walls.

In order to directly measure the central-cell ϕ_e and the barrier potential depression ϕ_b during both-end plugging, the Au neutral beams[14] are injected normally to the magnetic axis as is shown in Fig. 1. Beam-probe measurements have been made only on the axis in the present experiments. The plug potential ϕ_p's, as well as the parallel ion temperature at both ends, are deduced from energy analyses of the ions axially escaping through the plug potentials by use of ELA's. The axial potential profile is plotted in Fig. 1, together with profiles of density n and electron temperature T_e. The plug potential higher than the central one is created even with plug-to-central density ratio $n_p/n_c\sim0.5$ as long as n_p is larger than n_b. When the ratio n_p/n_b decreases, presumably because of ionization of neutral gas and collisional filling of central-cell cold ions in the barrier region, the potential differences among the plug, barrier, and central cell decrease, resulting in increased end losses. All of these results are consistent with the thermal-barrier concept.[5] The barrier-potential depression of 100–300 V agrees within a factor of 2 with theoretical prediction[15,16] for the central-cell T_{ec} in the range of 60–120 eV. ELA's cannot be used for plug-potential measurement for the case of too-strong plugging because of such small ion-end-loss fluxes. The maximum value of ion confining potential $\phi_c=\phi_p-\phi_e$ measured so far is about 1 kV.

Axial particle-confinement time for a core plasma $\tau_{\parallel}$ is obtained from the total ion number in the confining region divided by the integrated ion-loss fluxes to both ends. The core plasma is defined as the one within central-cell radius $r=10$ cm, half of the central-cell limiter radius 20 cm. The profiles of $n(r)$ and $j_{\parallel}(r)$ are measured with a scanning microwave interferometer and movable ELA's, of which the collecting efficiency is calibrated by use of Faraday cup. The

axial confinement time for the core plasma is plotted in Fig. 3 as a function of ϕ_c, together with the potential normalized by the parallel ion temperature $e\phi_c/T_{i\parallel}$. The solid line represents the theoretical prediction which includes both effects of collisional and collisionless (Pastukhov) confining scaling.[17] Here, two plug-to-central-cell mirror ratios $R = 2.5$ and 7.5 are employed corresponding to the location of the peak confining potential, expected to lie between the turning point of the sloshing ions (also near ω_{ce} resonance point) at 1 T and the plug mirror throat at 3 T. The experimentally obtained confinement time is in reasonable agreement with the theoretical scaling in the range of $1 < e\phi_c/T_{i\parallel} < 4$.

Nonambipolar radial ion losses, which are presumably associated with neoclassical ion transport, are estimated by measurement of the net current[18] flowing into the grounded end plates. The nonambipolar radial confinement time $\tau_\perp^{NA}$ for the core plasma is defined, similarly to $\tau_\parallel$, for $r \leqq = 10$ cm at the central-cell mapping to $r \leqq 70$ cm at the end plates. A limited data set so far obtained is plotted against the central-cell potential ϕ_e in Fig. 4. The data lie on the empirical formula

$$\tau_\perp^{NA} = 20[\phi_e/(1\text{ kV})]^{-1.0\pm0.3}\text{ ms},$$

for $\phi_e \geqslant 0.1$ kV, different from ϕ_e^{-2} dependence observed in TMX-U.[19] This result suggests that the transverse mobility coefficient is independent of radial electric field in the axisymmetrized field configuration. In the standard operation of GAMMA 10 the segmented end plates are floated so that the net current to the ends is effectively zero, i.e., $\tau_\perp^{NA}$ is considered to be longer than $\tau_\parallel$. This presumption is consistent with the following discussion on the ion particle balance. The potential ϕ_e is found to be decreased significantly by floating of the end plates.

Finally, ion particle balance is discussed in terms of the current balance equation

$$e\frac{dN}{dt} = I_{\text{ioniz}} - I_\perp^A - I_\perp^{NA} - I_\parallel.$$

Here, the total charge is $eN = 3.2\times10^{-2}$ C with the total number of particles $N = 2\times10^{17}$ in the core of the confining region with the effective length of 10.5 m. With the end plates floated, nonambipolar loss current $I_\perp^{NA}$ is negligible. In the quasisteady state of the central-cell density before plugging, the end-loss current $I_\parallel = 3$ A is equal to the difference between ionization source current I_{ioniz} and ambipolar loss current $I_\perp^A$. During strong end plugging, the end-loss current $I_\parallel$ is reduced to less than 0.3 A, and at the same time the increase of $e\,dN/dt = 3$ A is observed. Just after end plugging, the total ion number decays as $e\,dN/dt = -7$ A and the end loss $I_\parallel$ increases up to 10 A. These results indicate that $I_{\text{ioniz}} - I_\perp^A$ is kept nearly constant during the experimental shots and the density increase in the central cell is due to the end-loss reduction, namely, there is no enhanced radial transport driven by the increased potential.

In conclusion, results from the initial experiments in GAMMA 10 are as follows: (i) Thermal barrier and plug potentials are formed in axisymmetric end mirrors and confirmed from the direct measurements of potentials with beam probes. (ii) Axial profiles of the potential, density, and electron temperature are consistent with the prediction of thermal-barrier theory. (iii) Axial confinement time 100 times longer than the mirror confinement time has been attained by strong

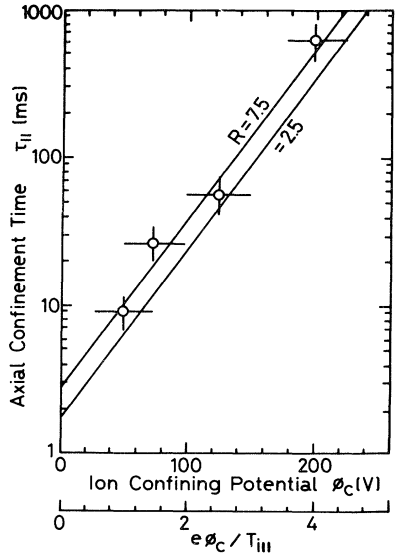

FIG. 3. Axial ion confinement time for core plasma vs ion confining potential ϕ_c and $e\phi_c/T_{i\parallel}$. Solid lines represent theoretical prediction.

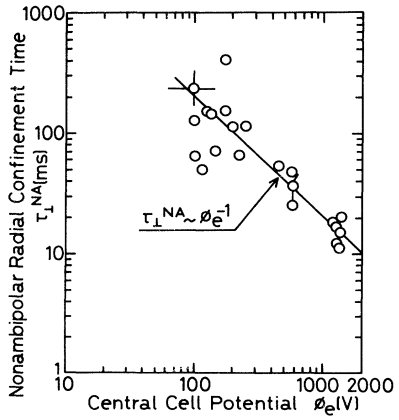

FIG. 4. Nonambipolar radial ion confinement time for core plasma vs central-cell potential ϕ_e. End plates are grounded for measurement of axial net current.

end plugging. Experimental scaling is in reasonable agreement with theoretical scaling for $1 < e\phi_c/T_{i\parallel} < 4$. (iv) Nonambipolar raidal ion confinement empirically scales as $\tau_\perp^{NA}(\mathrm{ms}) = 20\phi_e^{-1}$ (kV), indicating transverse mobility independent of radial electric field.

[1]K. Yatsu *et al.*, Phys. Rev. Lett. **43**, 627 (1979).

[2]S. Miyoshi *et al.*, in *Proceedings of the Eighth International Conference on Plasma Physics and Controlled Nuclear Fusion Research, Brussels, 1980* (International Atomic Energy Agency, Vienna, 1981), Vol. 1, p. 113.

[3]F. H. Coensgen *et al.*, Phys. Rev. Lett. **44**, 1132 (1980).

[4]R. Bruen *et al.*, Phys. Rev. Lett. **47**, 1833 (1981).

[5]D. E. Baldwin and B. G. Logan, Phys. Rev. Lett. **43**, 1318 (1979).

[6]D. P. Grubb *et al.*, Phys. Rev. Lett. **53**, 783 (1984).

[7]D. D. Ryutov and G. V. Stupakov, Fiz. Plazmy **4**, 50 (1978) [Sov. J. Plasma Phys. **4**, 278 (1978)].

[8]M. Inutake *et al.*, in *Fusion Reactor Design and Technology* (Unipub, New York, 1983), Vol. 1, p. 429.

[9]J. Kesner *et al.*, Nucl. Fusion **22**, 549 (1982).

[10]M. Inutake *et al.*, *Proceedings of the Ninth International Conference on Plasma Physics and Controlled Nuclear Fusion Research, Baltimore, 1982* (International Atomic Energy Agency, Vienna, 1983), Vol. 1, p. 545.

[11]G. V. Stupakov, Fiz. Plazmy **5**, 871 (1979) [Sov. J. Plasma Phys. **5**, 486 (1979)].

[12]T. Cho *et al.*, in *Proceedings of the Tenth International Conference on Plasma Physics and Controlled Nuclear Fusion Research, London, 1984* (International Atomic Energy Agency, Vienna, 1985), Vol. 2, p. 275.

[13]K. Yatsu *et al.*, Phys. Rev. Lett. **51**, 388 (1983).

[14]K. Ishii *et al.*, Rev. Sci. Instrum. **55**, 1924 (1984).

[15]R. H. Cohen *et al.*, Nucl. Fusion **20**, 1421 (1980).

[16]R. H. Cohen, Phys. Fluids **26**, 1977 (1983).

[17]T. D. Rognlien and T. A. Cutler, Nucl. Fusion **20**, 1003 (1980).

[18]E. B. Hooper *et al.*, Phys. Fluids **27**, 2264 (1984).

[19]T. C. Simonen *et al.*, in Ref. 12, Vol. 2, p. 255.